Synthesis of polyaniline based composite material and its analytical applications for the removal of highly toxic Hg^{2+} metal ion: Antibacterial activity against *E. coli*

Rani Bushra*, Mu. Naushad**,†, Gaurav Sharma***, Ameer Azam*, and Zeid Abdullah ALOthman**

*Department of Applied Physics, Aligarh Muslim University, Aligarh, India
**Advanced Materials Research Chair, Department of Chemistry, College of Science,
Bld#5, King Saud University, Riyadh-11451, Saudi Arabia
***School of Chemistry, Shoolini University, Solan, Himachal Pradesh, 173212, India

Abstract−A composite material polyaniline-Zr(IV) phosphoborate (PZPB) was synthesized via sol-gel method by the combination of Zr(IV) phosphoborate and polyaniline. The PZPB composite material was characterized by various analytical techniques. The PZPB composite material was found to be selective for Hg^{2+} metal ion due to the high distribution coefficient values for Hg^{2+} metal ion in all mediums. The PZPB composite material was used for Hg^{2+} removal under different experimental conditions. The antibacterial activity of PZPB composite material was also studied against *E. coli*.

Keywords: Polyaniline, Composite Material, Toxic Metals, Adsorption, Kinetics, Thermodynamics

INTRODUCTION

Water is recognized as source of evolution from origin to degree of human civilization. In the present scenario, with rapid increase in population growth, the world's population will reach nine billion by 2050, which will lead to a severe shortage of fresh water supply, so its treatment is a necessity for day to day life [1-3]. Residential areas, industrial waste, lack of adequate sanitation and continuous agricultural practices are the most significant forms of water pollution [4-7]. Nowadays, the pollution due to heavy metal ions is a serious ecological issue. Metal ions (Pb^{2+}, Cd^{2+}, As^{3+}, Cr^{3+}, Hg^{2+}) are considered to be more notorious water pollutants because these metal ions are non-biodegradable and hence are persistent in all parts of the environment [8-11]. Among all metal ions, Hg^{2+} is one of the most toxic metal ions [12-14]. There are various sources of Hg^{2+} ions in aquatic ecosystems, like paper and pulp manufacturing, oil refineries, chloralkali wastewater, power generation plants and fertilizers industries [15]. Mercury, which is present in different industrial waste effluents, has no positive impact on the human life; in fact, a safe level of its exposure is very difficult to determine. In the environment it is present in several different forms, and almost all forms are toxic [16].

Various techniques like chemical precipitation, flotation, coagulation-flocculation, adsorption, membrane filtration and ion-exchange have been used for the treatment of metal ions [17-21]. In recent years, adsorption of metal ions from contaminated water via composite ion exchange materials has been extensively studied [22-25] due to their certain characteristic properties such as better adsorption capacity, selectivity, functionality, chemical and thermal stability over their single component counterparts. Development of

composite material based on polyaniline (PANI) has gained interest [26]. Within the family of conducting polymers, PANI has attracted increased consideration due to its ease of preparation, high conductivity and good environmental stability, and its optical and electric properties can be reversibly controlled over an extensive range by both charge-transfer doping and protonation, which make this polymer appropriate matrix for synthesis of conducting polymer composites [27,28].

We have synthesized PZPB composite material which was used for Hg^{2+} removal from an aqueous medium. The as-prepared material was characterized properly using several analytical techniques. Batch studies were performed for the adsorption of Hg^{2+} ion from aqueous solution.

EXPERIMENTAL

1. Materials

Aniline, ammonium per sulfate, zirconium(IV) oxychloride, orthophosphoric acid and boric acid were supplied by E-Merck (India). All other reagents and chemicals were of analytical grade.

2. Sample Preparation

Polyaniline was prepared from monomer of aniline (10%) and ammonium per sulfate as oxidant by using oxidative polymerization method as described previously [29,30]. Solutions of boric acid (0.1 M) and orthophosphoric acid (0.1 M) were prepared in distilled water with varying volume ratios and added to zirconium (IV) oxychloride (0.1 M) under constant stirring for 1 h. A white gel type slurry of Zr(IV) phosphoborate was obtained after adjusting the pH of the mixture with nitric acid or ammonia solution. In the resulting mixture, polyaniline gel was added with continuous stirring and kept for 24 hrs for digestion. Afterwards, the precipitate was filtered, washed with DMW and dried at 50±2 °C. PZPB composite material was converted into H$^+$ form by treating it with 1 M nitric acid, then further filtered again by suction filtration, washed

thoroughly with DMD and dried at 50±2 $^{\circ}$C.

3. Characterization

The morphology of the PZPB composite was studied with SEM (LEO, 435 VF). The FTIR analysis was performed on FTIR spectrometer (Perkin Elmer 1730, USA) using the KBr disc method. The XRD of PZPB was taken using X'Pert PRO analytical diffractometer (PW-3040/60 Netherlands with CuKa radiation l=1.5418 A$^{\circ}$). Thermogravimetric analysis was carried out on an automatic thermal analyzer (V2.2A Du Pont 9900) in the N$_2$ atmosphere.

4. Physiochemical Properties

The capability of adsorption and the nature of functional group present on the PZPB composite material were determined by ion exchange capacity and pH titrations. Elution behavior was accomplished for the elution of H$^+$ ions from the PZPB composite material. The optimal concentration required for the complete removal of H$^+$ ion was also determined [31].

5. Distribution Coefficient Studies (K$_d$)

The K$_d$ values of various metal ions were evaluated by batch method in different solvent systems by the method described elsewhere [32-34]. The concentration of metal ion before and after adsorption was evaluated by EDTA titrations. The distribution coefficient values are calculated as:

$$K_d = \frac{\text{Amount of metal ion retained in one gram of the exchanger phase (mgg}^{-1})}{\text{Amount of metal in unit volume of the supernatant solution (mgmL}^{-1})} \quad (1)$$

6. Batch Adsorption Experiments

A batch method was applied for the adsorption of Hg^{2+} onto PZPB composite material. For this study, 100 mg of PZPB was stirred with 250 mL of Hg^{2+} solution of known concentration for different time periods at room temperature. Then, PZPB was filtered off and the concentration of Hg^{2+} in the solution phase was evaluated by EDTA titration. Different adsorption parameters were also optimized.

The removal efficiency of Hg^{2+} adsorption was calculated as:

$$q_e = \frac{(C_o - C_e)V}{m} \quad (2)$$

Kinetics studies were accomplished by changing the Hg^{2+} concentration (C$_o$, 20, 30 and 50 μg L^{-1}). Isotherm and thermodynamic studies were performed by varying the temperature (25-45 $^{\circ}$C) and initial Hg^{2+} concentration (20-100 mg L^{-1}).

7. Antibacterial Activity Against E. coli

The antibacterial nature of PZPB composite material was determined against *E. coli* by employing optical density method. The *E. coli* was cultured overnight in agar plate; a colony of *E.coli* was picked

form plate and inoculated into 10 mL of nutrient broth. The inoculum was then incubated at 37 $^{\circ}$C for 24 hrs. Finally, the culture was diluted to 10^{-5} CFU/mL (colony forming unit per mL) according to the MacFarland standard using nutrient broth [3,35,36]. The above culture was taken in four flasks and different concentrations (50, 100, 200, 300 μg/mL) of PZPB composite material were added to these flasks. The flasks were then again incubated in an incubator shaker for 24 hrs at 37 $^{\circ}$C. To reduce aggregation and settlement of the PZPB composite, during the incubation period high rotation was performed for each flask. The positive control was also set up simultaneously, which showed growth of *E. coli* in absence of PZPB composite material. The optical density of each flask was evaluated after every hour with a spectrophotometer at 620 nm. Finally, the optical density (O.D.) was plotted against time of incubation [37]. Further, the disc diffusion method was used for confirming the antibacterial nature of PZPB composite material. The different concentrations of PZPB composite as used in optical density method were taken. Nutrient agar medium was autoclaved at 15 psi and 121 $^{\circ}$C, and from this about 10-20 mL of nutrient agar medium was poured into sterilized petri dish and left for solidification. After solidification, the petri dish was inoculated with suspension of *E. coli* by spread plate method. Paper discs were made and dipped in different concentration solutions of PZPB composite and placed in a petri dish. Finally, the petri dish was sealed with paraffin and incubated at 37 $^{\circ}$C. The petri dish was studied to find the zone of inhibition after 24-48 hrs.

RESULTS AND DISCUSSION

Different samples of PZPB composite material with varying volume ratios were prepared by sol gel method at pH 1, because there is a possibility of hydrolysis of the material at higher pH (Table 1). It is evident from Table 1 that the yield and ion exchange capacity (IEC) of the material was affected by the mixing ratios of the reactants. It was noted that the ion exchange capacity was increased with increasing the ratio of the anionic parts in the reaction mixture as the replaceable hydrogen/ionogenic groups were attached to these anionic groups [25,38,39]. Among the various samples, the IEC for Na$^+$ was maximum for sample M-3; therefore, it was chosen for thorough studies.

The gel of polyaniline was prepared by oxidative coupling using K$_2$S$_2$O$_8$ in acidic medium [40] as:
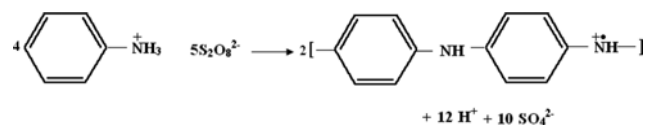

**Table 1. Conditions for the synthesis of PZPB composite material**

S. no.	A (Mol L^{-1})	B (Mol L^{-1})	C (Mol L^{-1})	D (Percentage)	Mixing ratio (V/V)	pH	IEC for Na$^+$ ions (meq g^{-1})	Yield (g)
M-1	0.10	0.10	0.10	10%	1 : 1 : 1 : 1	1.0	1.0	6.57
M-2	0.10	0.10	0.10	10%	1 : 2 : 1 : 1	1.0	1.25	7.00
M-3	0.10	0.10	0.10	10%	1 : 2 : 2 : 1	1.0	1.50	7.54
M-4	0.10	0.10	0.10	10%	2 : 2 : 1 : 1	1.0	0.52	7.44

A: Zirconium (IV)oxychloride, B: Boric acid, C: Orthophosphoric acid , D: Polyaniline , IEC: Ion exchange capacity

Table 2. Ion exchange capacity of various metal ions on PZPB

Exchanging ions	Li^+	Na^+	K^+	Mg^{2+}	Ca^{2+}	Sr^{2+}	Ba^{2+}
IEC (meq g^{-1})	0.80	1.50	1.62	0.72	1.00	1.08	1.67

Zr(IV) phosphoborate and polyaniline binding can be shown as:
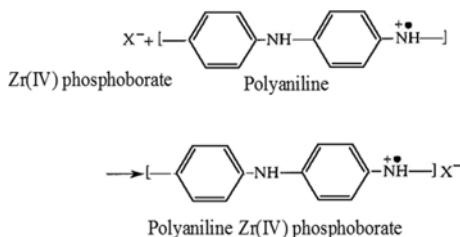
The affinity order for some monovalent and divalent cations (Table 2) was $Li^+ < Na^+ < K^+$ and $Mg^{2+} < Ca^{2+} < Sr^{2+} < Ba^{2+}$ which was in agreement with the size of hydrated ionic radii of the exchanging ions [41].

The pH titration curve of some metal halides and their corresponding hydroxides showed the bifunctional behavior of the PZPB

(Fig. 1(a)). It is evident from Fig. 1(b) that 1.0 M NaNO$_3$ was appropriate as eluent for the full release of H^+ ions from the composite material. From elution behavior, it was confirmed that only 70 mL of 1.0 M NaNO$_3$ solution was enough for the maximum elution of H^+ ions, which indicated the significant efficiency of the column (Fig. 1(c)).

The sorption behavior of the composite material was determined by distribution coefficient (K_d) values. It is observed from Table 3 that sorption of metal ion was increased with decreasing the concentration of the acids. The low K_d values of all metal ions in high acidic medium was due to the occurrence of high concentration of H^+ ions, which inverted the adsorption process and the regeneration process dominated over the adsorption process. The PZPB composite was found to be selective for Hg^{2+} metal ions because its uptake was high in all solvents as compared to other metal ions.

In the FTIR spectra of PZPB composite material (Fig. 2(a)), the bands in the region of 1,565 and 1,489 cm^{-1} are ascribed due to C=N stretching mode of quinoid (Q) rings and C=C stretching mode of benzenoid (B) rings, respectively [42,43]. Bands at 1,306 and 1,243 cm^{-1} reveal the presence of methylene group. The presence of the phosphate group in the composite material is confirmed by the
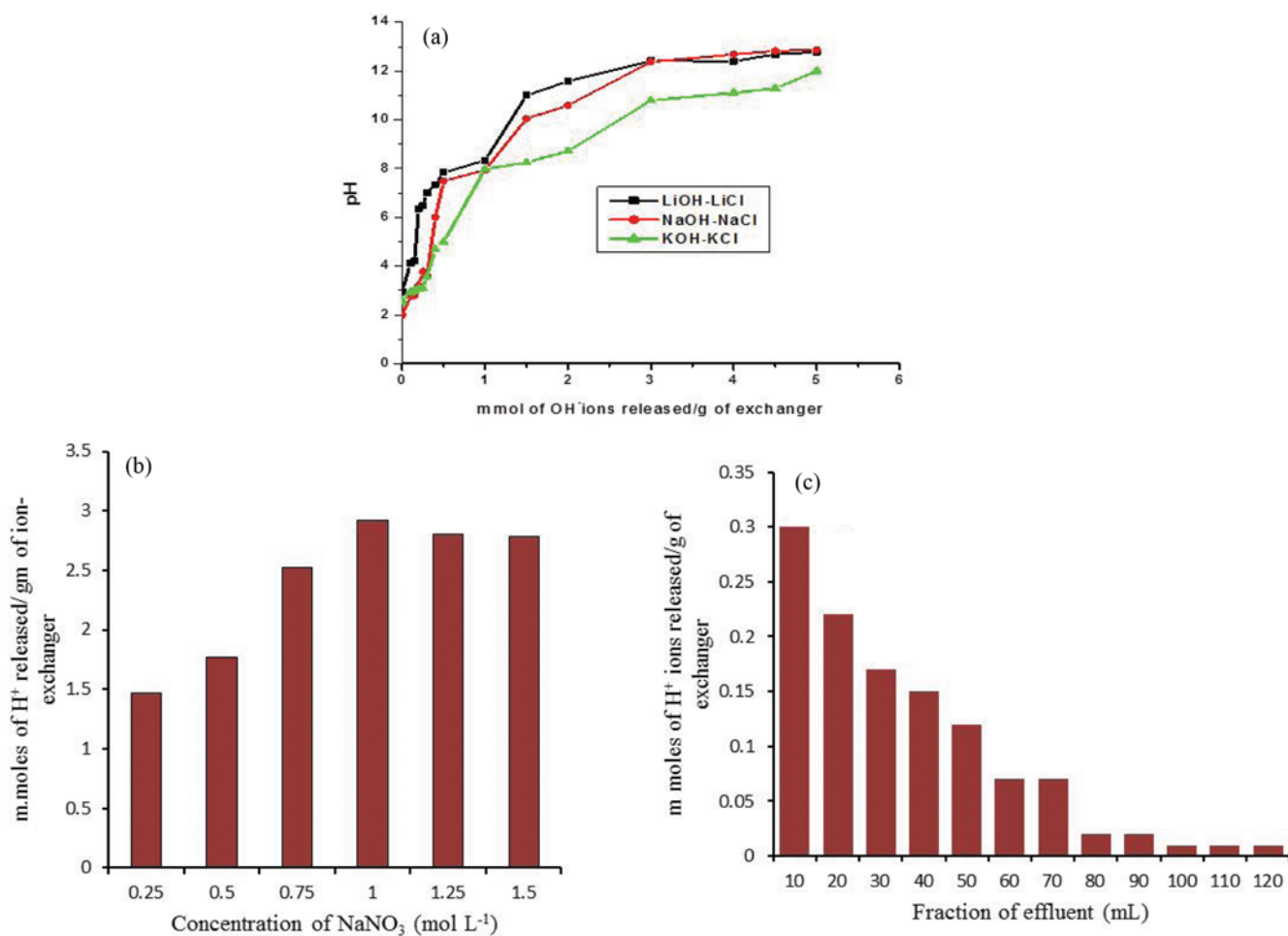

Fig. 1. (a) pH titration of PZPB with various alkali metal hydroxides (b) effect of eluent concentration on IEC of PZPB (c) effect of eluent concentration on IEC of PZPB.
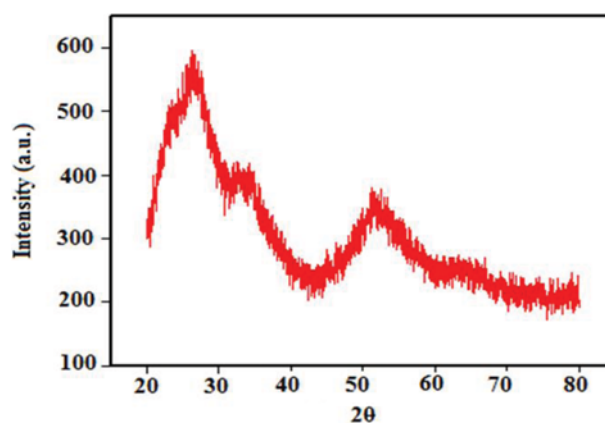
Table 3. K_d values of metal ions on PZPB composite material in different solvent systems

Metal ion	DMW	HNO_3 (1 M)	HNO_3 (0.1 M)	HNO_3 (0.01 M)	$HClO_4$ (1 M)	$HClO_4$ (0.1 M)	$HClO_4$ (0.01 M)
Mg^{2+}	10.0	58	200	487	28	157	183
Zn^{2+}	3.5	28	47	145	24	46	138
Pb^{2+}	21	48	110	300	280	850	1100
Cd^{2+}	31	347	410	590	389	473	739
Cu^{2+}	43	45	110	300	30	82	340
Ni^{2+}	225	347	260	410	389	478	739
Hg^{2+}	**500**	**559**	**1570**	**2900**	**870**	**1402**	**1808**
Er^{3+}	32	135	329	583	220	289	370
Ce^{3+}	57	60	138	600	98	198	350
Nd^{3+}	35	180	300	550	162	350	410
Y^{3+}	92	63	658	182	158	480	410
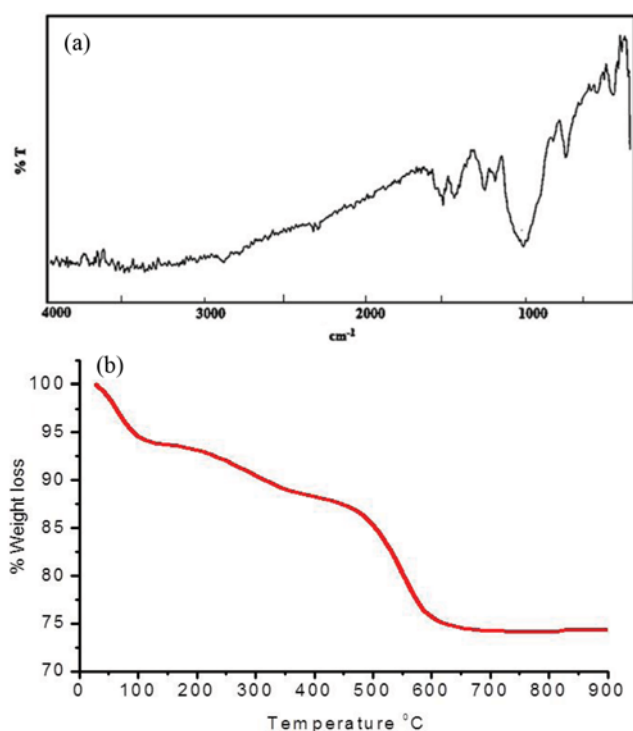
Fig. 2. (a) FTIR spectrum and (b) TGA of PZPB composite material.

Fig. 3. Powder X-ray diffraction pattern of PZPB composite material.

The X-ray diffractogram (Fig. 3) of PZPB composite material shows its semi-crystalline nature due to a number of low intense peaks.

Surface morphology of inorganic part (Zr(IV) phosphoborate) and PZPB composite material is shown in Fig. 4(a), (b). The SEM images clearly exhibit that the surface morphology of PZPB was totally dissimilar from its individual inorganic component. The morphology of the PZPB revealed that the polyaniline gets deposited over and between Zr(IV) phosphoborate. The EDX spectrum of Zr(IV) phosphoborate gave the peaks of B, O, P, and Zr. But, the EDX spectrum of PZPB composite material showed two additional peaks for C and N, which confirmed the mixing of PANI with Zr(IV) phosphoborate.

For the optimum adsorption of Hg^{2+}, the equilibration time was achieved at diverse time intervals (5-240 min), and it was found that adsorption was fast at the starting and equilibrium was achieved within 180 min at which 86.3% Hg^{2+} was adsorbed onto PZPB composite material (Fig. 5(a)). Actually, all sites at the PZPB surface were vacant at the start, so the adsorption was fast [7,38,48, 49]. Later, due to the decrease in the Hg^{2+} concentration as well as the number of adsorption sites at PZPB, the adsorption became slow [2,50]. In the pH effect, the Hg^{2+} adsorption increased from 29.8 to 86% with increasing the pH from 2 to 6 (Fig. 5(b)). After pH 6, the adsorption of Hg^{2+} was not changed because at pH>6.0,

presence of the band at 1,068 cm^{-1} [44]. Finally, the bands at ~802 and 512 cm^{-1} show the superposition of metal oxygen stretching vibrations [45].

TGA study was done to determine the thermal stability of the PZPB composite material. The results reveal three-step weight loss behavior (Fig. 2(b)). The first weight loss (10%) up to 150 °C was due to the loss of external H_2O molecule from the PZPB composite material [46]. The second weight loss onwards in the range from 200 to 350 °C corresponded to the elimination of interstitial H_2O molecules as well as change of phosphate group to pyrophosphate group [47]. Further loss in weight up to 500 °C might be allocated to the decomposition of organic part of the composite material. Afterward, there was no weight loss up to 900 °C because of the change of the material into its corresponding oxides and might be due to carbonization of polyaniline.
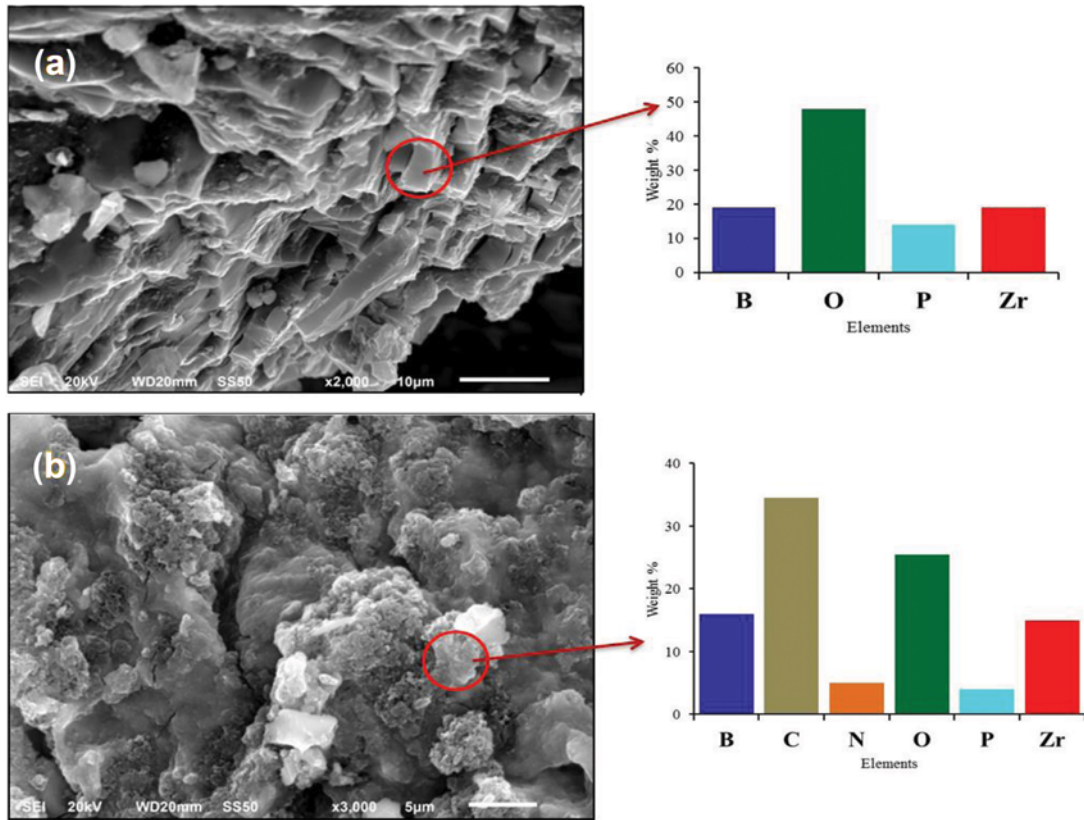
Fig. 4. SEM-EDX images for (a) Zr(IV) phosphoborate and (b) PZPB composite composite material.
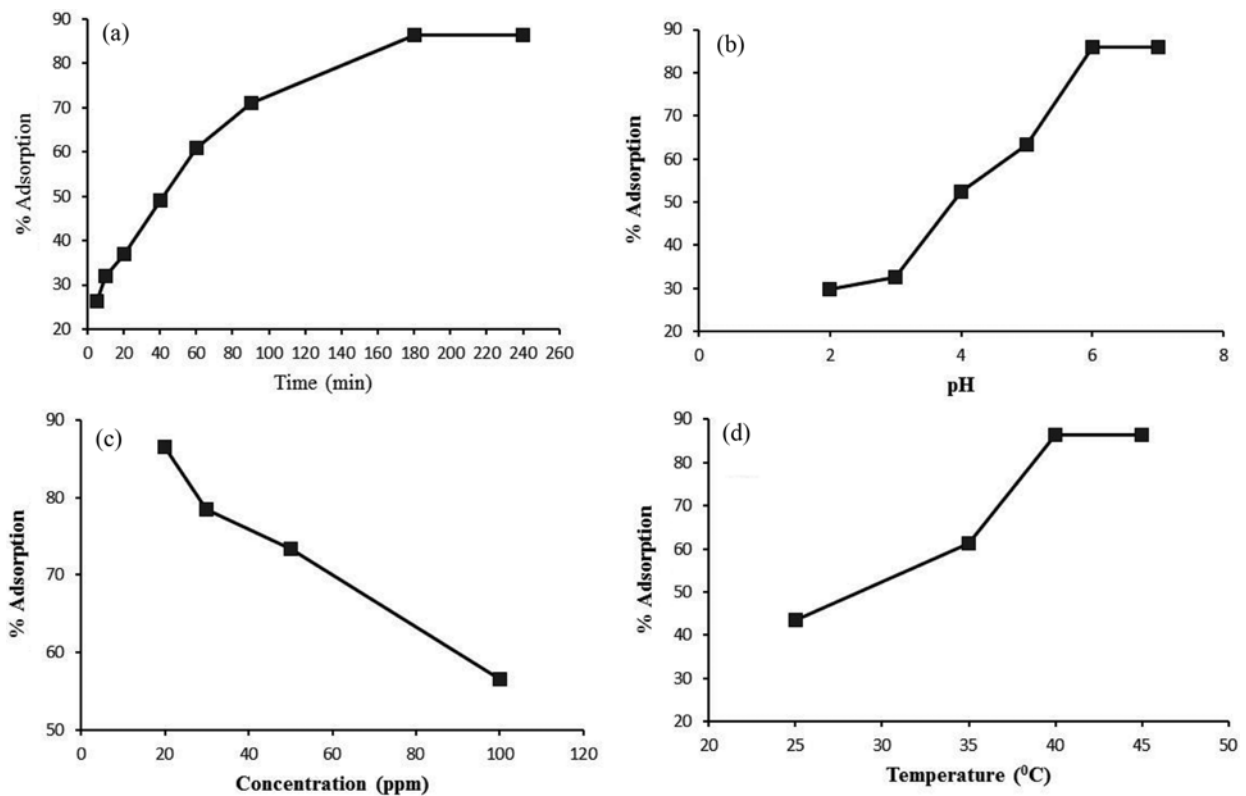

Fig. 5. Percent removal of Hg^{2+} metal ion using PZPB composite material at different (a) time, (b) pH, (c) Initial Hg^{2+} metal ion concentration and (d) temperature.

the Hg^{2+} metal ion gets precipitated [50]. As anticipated, the removal of Hg^{2+} was low at lower pH. Actually, the H^{+} ions concentration was high at lower pH, due to which the protonation of active sites of PZPB was dominated over the adsorption process. In the concentration effect, the adsorption of Hg^{2+} was decreased from 86.5 to 56.5% with increasing in the concentration of Hg^{2+} from 20 to 100 mg L^{-1} (Fig. 5(c)). The decrease in the adsorption percentage of Hg^{2+} metal ion was due to the less availability of adsorption sites at the surface of PZPB for the higher concentration of Hg^{2+} metal ion. The synthesis and the adsorption of Hg^{2+} onto PZPB are shown in Fig. 6.

1. Adsorption Kinetics and Isotherm Studies

The adsorption of Hg^{2+} onto PZPB was evaluated by pseudo-first-order and pseudo-second-order kinetic models [51,52] and Lang-

muir and Freundlich isotherm models [53,54].

The pseudo-first-order and pseudo-second-order equations are represented as follows:

Pseudo-first-order:

$$\log(q_e - q_t) = \log q_e - \frac{k_1 t}{2.303} \tag{3}$$

Pseudo-second-order:

$$\frac{t}{q_t} = \frac{1}{k_2 q_e^2} + \frac{t}{q_e} \tag{4}$$

It is clear from Table 4 that the values of R^2 for pseudo-first-order model were higher than pseudo-second-order model, which indicated that the studied adsorption system fits to the pseudo-first-
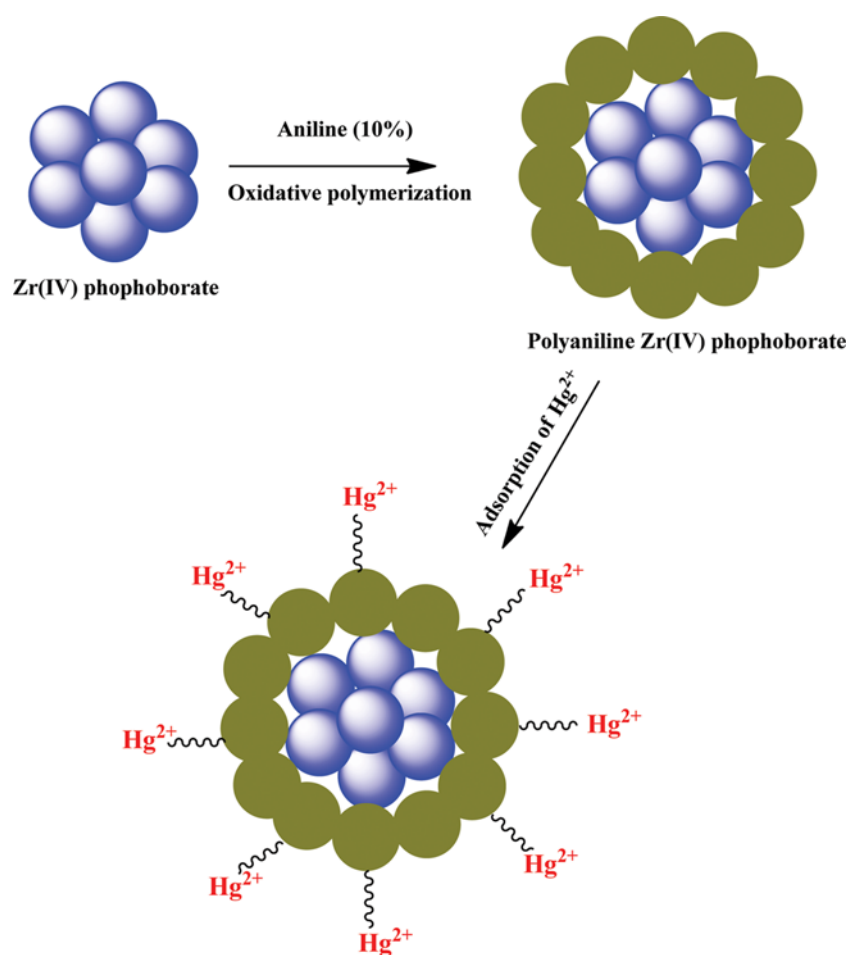

Fig. 6. Scheme for the synthesis of PZPB and adsorption of Hg^{2+} onto PZPB.

Table 4. Kinetic parameters for the adsorption of Hg^{2+} onto PZPB

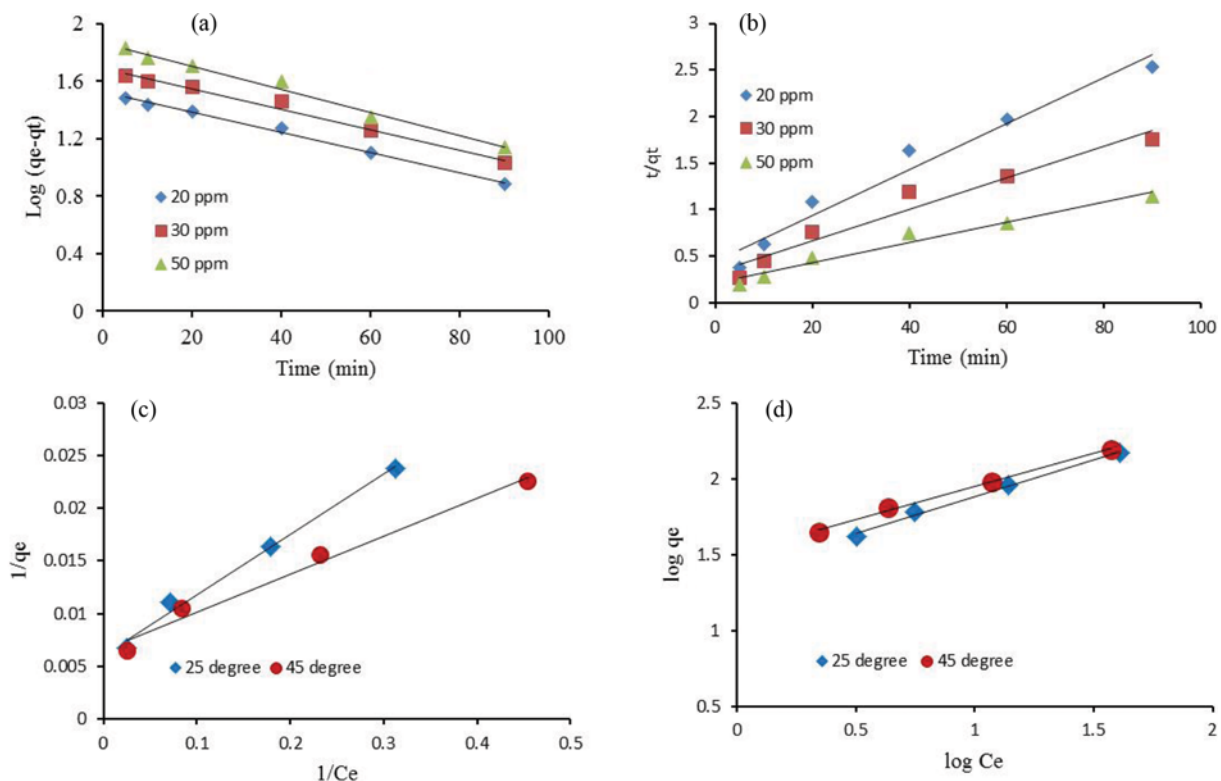| Kinetic models	Parameters	20 ppm	30 ppm	50 ppm
Pseudo-first-order	k_1 (min^{-1})	1.61×10^{-2}	1.56×10^{-2}	0.92×10^{-2}
	R^2	0.994	0.990	0.981
Pseudo-second-order	q_e (mg g^{-1})	40.48	59.17	92.59
	k_2 (g mg^{-1} min^{-1})	1.37×10^{-3}	0.87×10^{-3}	0.54×10^{-3}
	R^2	0.965	0.952	0.966

Fig. 7. Plots of (a) Pseudo-first-order, (b) Pseudo-second-order (c) Langmuir isotherm and (d) Freundlich isotherm models.

order kinetic model (Fig. 7(a), 7(b)).

The Langmuir isotherm model is given as:

$$\frac{1}{q_e} = \frac{1}{q_m} + \frac{t}{bq_mC_e} \tag{5}$$

A dimensionless equilibrium parameter (R_L) is given as [55]:

$$R_L = \frac{1}{1+bC_o} \tag{6}$$

Freundlich isotherm is expressed by the following equation:

$$\log q_e = \log K_f + \frac{1}{n}\log C_e \tag{7}$$

The values of q_m increased with increasing the temperature, which exhibited the endothermic nature for the Hg^{2+} adsorption

Table 5. Isotherm model parameters for Hg^{2+} adsorption of onto PZPB

Equilibrium model	Parameters	25 °C	45 °C
Langmuir isotherm	q_m (mg g^{-1})	153.85	163.93
	b (L mg^{-1})	11.4×10^{-2}	16.9×10^{-2}
	R_L	0.30	0.22
	R^2	0.990	0.982
Freundlich isotherm	K_f (L mg^{-1})	25.1	32.6
	n	2.08	2.32
	R^2	0.995	0.997

onto PZPB (Table 5). The values of $R_L < 1$ indicated the promising adsorption of Hg^{2+} onto PZPB. The parameters obtained by fit-

Table 6. A list of maximum monolayer adsorption capacity for Hg^{2+} using various adsorbents

Adsorbents	Maximum monolayer adsorption capacity (mg g^{-1})	References
4-Aminoantipyrine immobilized bentonite	52.9	[56]
Mesoporous silica-coated magnetic particles	14	[57]
Coconut shell activated carbon	15	[58]
Coal	10	[59]
Ti(IV) iodovanadate	21.32	[6]
Chemically treated sawdust (Acacia arabica)	20.62	[60]
2-Mercaptobenzothiazole treated clay	2.71	[61]
Bamboo	2.71	[62]
PZPB	153.85	Present work

ting these two isotherm models (Fig. 7(c), 7(d)) are given in Table 5. The Freundlich isotherm model showed the better correlation coefficient values (R^2>0.98) than Langmuir isotherm model, which indicates the superior applicability of this model.

A comparison of q$_m$ of Hg^{2+} on various adsorbents is shown in Table 6 [6,56-62]. The value of q$_m$ for PZPB was higher than most of the adsorbents shown in Table 6.

2. Thermodynamic Studies

From the thermodynamic studies (Fig. 5(d)), adsorption of Hg^{2+} was increased from 42.3 to 85.6% on increasing the temperature from 25 to 45 °C. The effect of temperature on the adsorption is also related to other parameters: ΔG^o, ΔH^o and ΔS^o. The values of ΔH^o and ΔS^o were found from the slopes and intercepts of the plots of lnK$_c$ versus 1/T by this equation:

$$\ln K_c = -\frac{\Delta H^o}{RT} + \frac{\Delta S^o}{R} \tag{8}$$

The values of ΔG^o were calculated as:

$$\Delta G^o = \Delta H^o - T\Delta S^o \tag{9}$$

The positive value of ΔH^o indicates the endothermic nature of adsorption (Table 7). The positive values ΔS^o showed an increase in the randomness. The ΔG^o values were negative which showed the degree of spontaneity of the adsorption process.

3. Antibacterial Activity of PZPB Composite Material Against E. coli

The antibacterial activity of PZPB composite material was studied against E. coli. The inhibition of bacterial growth can be clearly seen in growth curves (Fig. 8(a)). The growth curves studies of E. coli proved the bacteriostatic nature of PZPB composite material. It was revealed that a concentration of 300 μg/mL of composite totally stopped the growth of E. coli for the 24 hrs. The other con-

centration of PZPB composite material was also found effective to stop the growth of bacteria and has bacteriostatic nature but to a lesser extent. The death phase of the E. coli was observed after 22 hrs of incubation. The presence of Zr metal ion in the composite might be responsible for lysis of E. coli bacterial cellular membranes. The interactions between the PZPB composite material and bacterial cells might be responsible for the disruption of the cell membrane by oxidative-reductive decomposition of functional groups in the proteins presents on the outer surface of cell membranes [63,64]. The disc diffusion method also proved the inhibitory nature of PZPB composite material with maximum inhibition zone of 21 mm for 300 μg/mL and 16 mm for 50 μg/mL, 17 mm for 100 μg/mL, 19 mm for 200 μg/mL, respectively (Fig. 8(b)).

CONCLUSION

PZPB composite material was synthesized by the combination of inorganic Zr(IV) phosphoborate and polyaniline via sol-gel method. The material was characterized by various analytical techniques. The X-ray diffractogram of PZPB composite material showed the semi-crystalline nature of the material. The morphology of the composite material (SEM) showed the polyaniline gets deposited over and between Zr(IV) phosphoborate. The PZPB composite material was successfully used for the removal of Hg^{2+} metal ion from aqueous medium. The highest adsorption was at pH 6 and equilibration was attained within 180 min. The adsorption of Hg^{2+} onto PZPB was endothermic. The antibacterial activity of PZPB composite material was studied against E. coli. The disc diffusion method also proved the inhibitory nature of PZPB composite material with maximum inhibition zone of 21 mm for 300 μg/mL and 16 mm for 50 μg/mL, 17 mm for 100 μg/mL, and 19 mm for 200 μg/mL, respectively.

Table 7. Thermodynamics parameters for Hg^{2+} adsorption onto PZPB

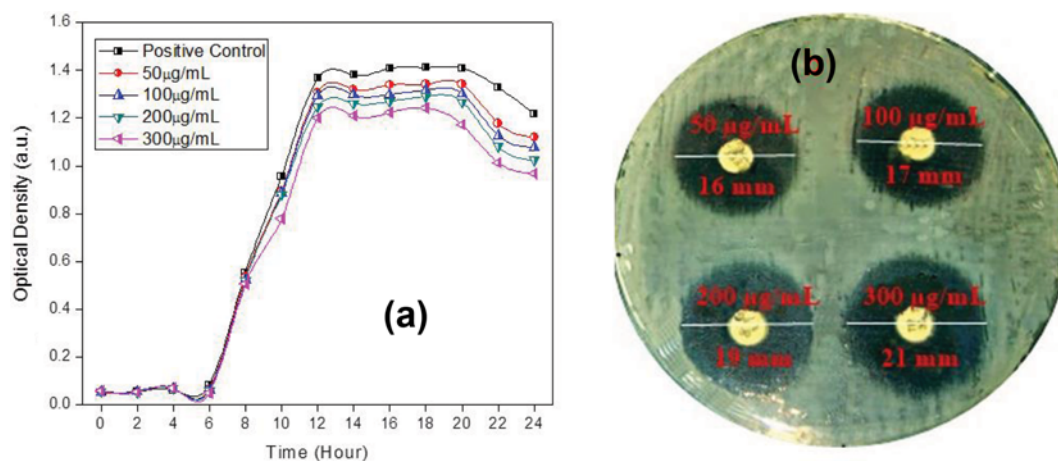| C$_o$ (mg L^{-1})	ΔH^o (KJ mol^{-1})	ΔS^o (KJ mol^{-1} K^{-1})	$-\Delta G^o$ (KJ mol^{-1})			
			298 K	308 K	313 K	318 K
50	8.29	0.035	2.14	2.49	2.67	2.84

Fig. 8. (a) Growth curve of E. coli in presence of PZPB (b) antibacterial activity PZPB against E. coli using disc diffusion method.

REFERENCES

1. Z. A. ALOthman and M. Naushad, *Des. Water Treat*, **53**, 2158 (2105).
2. A. A. Alqadami, M. Naushad, M. A. Abdalla, T. Ahamad, Z. A. ALOthman and S. M. Alshehri, *RSC Adv.*, **6**, 22679 (2016).
3. G. Sharma, A. Kumar, M. Naushad, D. Pathania and M. Sillanpää, *J. Ind. Eng. Chem.*, **33**, 201 (2016).
4. M. Naushad, T. Ahamad, Z. A. ALOthman, M. A. Shar, N. S. AlHokbany and S. M. Alshehri, *J. Ind. Eng. Chem.*, **29**, 78 (2015).
5. M. Naushad, Z. A. ALOthman, G. Sharma and Inamuddin, *Ionics (Kiel)*, **21**, 1453 (2015).
6. M. Naushad, Z. A. ALOthman, M. R. Awual, M. M. Alam and G. E. Eldesoky, *Ionics (Kiel)*, **21**, 2237 (2015).
7. A. Shahat, M. R. Awual, M. A. Khaleque, M. Z. Alam, M. Naushad and A. M. S. Chowdhury, *Chem. Eng. J.*, **273**, 286 (2015).
8. L. K. Wang, *Industrial and Hazardous Waste Treatment*, Van Nostrand Reinhold, New York (2006).
9. C.-G. Lee, S. Lee, J.-A. Park, C. Park, S. J. Lee, S.-B. Kim, B. An, S.-T. Yun, S.-H. Lee and J.-W. Choi, *Chemosphere*, **166**, 203 (2017).
10. C.-H. Yen, H.-L. Lien, J.-S. Chung and H.-D. Yeh, *J. Hazard. Mater.*, **322**, 215 (2017).
11. S. Zhang, H. Gao, J. Li, Y. Huang, A. Alsaedi, T. Hayat, X. Xu and X. Wang, *J. Hazard. Mater.*, **321**, 92 (2017).
12. C. Xiong, Y. Li, G. Wang, L. Fang, S. Zhou, C. Yao, Q. Chen, X. Zheng, D. Qi, Y. Fu and Y. Zhu, *Chem. Eng. J.*, **259**, 257 (2015).
13. Z. Wang, J. Xu, Y. Hu, H. Zhao, J. Zhou, Y. Liu, Z. Lou and X. Xu, *J. Taiwan Inst. Chem. Eng.*, **60**, 394 (2016).
14. N. Saman, K. Johari, S.-T. Song, H. Kong, S.-C. Cheu and H. Mat, *Chemosphere*, **171**, 19 (2017).
15. B. Henriques, C. B. Lopes, P. Figueira, L. S. Rocha, A. C. Duarte, C. Vale, M. A. Pardal and E. Pereira, *Chemosphere*, **171**, 208 (2017).
16. M. R. Awual, M. M. Hasan, G. E. Eldesoky, M. A. Khaleque, M. M. Rahman and M. Naushad, *Chem. Eng. J.*, **290**, 243 (2016).
17. S. Wernisch, O. Trapp and W. Lindner, *Anal. Chim. Acta*, **795**, 88 (2013).
18. T. A. Kurniawan, G. Y. S. Chan, W.-H. Lo and S. Babel, *Chem. Eng. J.*, **118**, 83 (2006).
19. F. Fu and Q. Wang, *J. Environ. Manage.*, **92**, 407 (2011).
20. Y.-H. Wang, S.-H. Lin and R.-S. Juang, *J. Hazard. Mater.*, **102**, 291 (2003).
21. D. W. O'Connell, C. Birkinshaw and T. F. O'Dwyer, *Bioresour. Technol.*, **99**, 6709 (2008).
22. S. A. Nabi, M. Shahadat, R. Bushra, M. Oves and F. Ahmed, *Chem. Eng. J.*, **173**, 706 (2011).
23. R. Bushra, M. Naushad, R. Adnan, Z. A. ALOthman and M. Rafatullah, *J. Ind. Eng. Chem.*, **21**, 1112 (2015).
24. R. Bushra, M. Shahadat, A. Ahmad, S. A. Nabi, K. Umar, M. Oves, A. S. Raeissi and M. Muneer, *J. Hazard. Mater.*, **264**, 481 (2014).
25. S. A. Nabi, M. Naushad and R. Bushra, *Chem. Eng. J.*, **152**, 80 (2009).
26. Inamuddin, S. A. Khan, W. A. Siddiqui and A. A. Khan, *Talanta*, **71**, 841 (2007).
27. S. Roth and W. Graupner, *Synth. Met.*, **57**, 3623 (1993).
28. S. B. Kondawar, S. R. Thakare, V. Khati and S. Bompilwar, *Int. J. Mod. Phys. B*, **23**, 3297 (2009).
29. M. Naushad, Inamuddin and T. A. Rangreez, *Des. Water Treat.*, **55**, 463 (2015).
30. P. Bandyopadhyay, T. Kuila, J. Balamurugan, T. T. Nguyen, N. H. Kim and J. H. Lee, *Chem. Eng. J.*, **308**, 1174 (2017).
31. S. A. Nabi, R. Bushra, Z. A. ALOthman and M. Naushad, *Sep. Sci. Technol.*, **46**, 847 (2011).
32. Z. A. ALOthman, M. Naushad and Inamuddin, *Chem. Eng. J.*, **172**, 369 (2011).
33. Z. A. ALOthman, Inamuddin and M. Naushad, *Chem. Eng. J.*, **171**, 456 (2011).
34. Z. A. ALOthman, M. M. Alam and M. Naushad, *J. Ind. Eng. Chem.*, **19**, 956 (2013).
35. M. J. Hajipour, K. M. Fromm, A. A. Ashkarran, D. J. de Aberasturi, I. R. de Larramendi, T. Rojo, V. Serpooshan, W. J. Parak and M. Mahmoudi, *Trends Biotechnol.*, **31**, 61 (2016).
36. G. Sharma, D. Pathania and M. Naushad, *J. Ind. Eng. Chem.*, **20**, 4482 (2014).
37. D. Pathania, G. Sharma, A. Kumar, M. Naushad, S. Kalia, A. Sharma and Z. A. ALOthman, *Toxicol. Environ. Chem.*, **97**, 526 (2015).
38. S. A. Nabi and M. Naushad, *Colloids Surfaces A Physicochem. Eng. Asp.*, **316**, 217 (2008).
39. S. A. Nabi and M. Naushad, *Colloids Surfaces A Physicochem. Eng. Asp.*, **293**, 175 (2007).
40. M. Naushad, Z. A. ALOthman and M. Islam, *Int. J. Environ. Sci. Technol.*, **10**, 567 (2013).
41. A. M. K. S. A. Nabi, *Ann. Chim. Sci. Mater.*, **21**, 521 (1996).
42. C. W. Lin, B. J. Hwang and C. R. Lee, *Mater. Chem. Phys.*, **58**, 114 (1999).
43. A. Choudhury, *Sensors Actuators B Chem.*, **138**, 318 (2009).
44. C. N. R. Rao, *Chemical Applications of Infrared Spectroscopy*, Academic Press, New York (n.d.).
45. K. Nakamoto, *Infrared and Raman Spectra of Inorganic and Coordination Compounds Part B: Applications in Coordination, Organometallic, and Bioinorganic Chemistry*, 6th Ed., John Wiley and Sons, New York (1986).
46. C. Duval, *Inorganic Thermogravimetric Analysis*, Elsevier, Amsterdam (1963).
47. A. A. Khan and T. Akhtar, *Electrochim. Acta*, **53**, 5540 (2008).
48. A. B. Albadarin, M. N. Collins, M. Naushad, S. Shirazian, G. Walker and C. Mangwandi, *Chem. Eng. J.*, **307**, 264 (2017).
49. M. Naushad, S. Vasudevan, G. Sharma, A. Kumar and Z. A. ALOthman, *Desalin. Water Treat.*, **57**, 18551 (2016).
50. M. Naushad, T. Ahamad, G. Sharma, A. H. Al-Muhtaseb, A. B. Albadarin, M. M. Alam, Z. A. ALOthman, S. M. Alshehri and A. A. Ghfar, *Chem. Eng. J.*, **300**, 306 (2016).
51. Y. S. Ho, G. Mckay, D. A. J. Wase and C. F. Foster, *Ads. Sci. Tech.*, **18**, 639 (2000).
52. Lagergren S. and K. Sven, Vetenskapsakademiens Handl, **24**, 1 (1898).

53. I. Langmuir, *J. Am. Chem. Soc.*, **40**, 1361 (1918).
54. H. M. F. Freundlich, *J. Phys. Chem.*, **57**, 385 (1906).
55. S. M. Alshehri, M. Naushad, T. Ahamad, Z. A. ALOthman and A. Aldalbahi, *Chem. Eng. J.*, **254**, 181 (2014).
56. Q. Wang, X. Chang, D. Li, Z. Hu, R. Li and Q. He, *J. Hazard. Mater.*, **186**, 1076 (2011).
57. J. Dong, Z. Xu and F. Wang, *Appl. Surf. Sci.*, **254**, 3522 (2008).
58. J. Karthikeyan and M. Chaudhuri, *Water Res.*, **20**, 449 (1986).
59. A. K. Meena, K. Kadirvelu, G. K. Mishra, C. Rajagopal and P. N. Nagar, *J. Hazard. Mater.*, **150**, 604 (2008).
60. D. M. Manohar, K. A. Krishnan and T. S. Anirudhan, *Water Res.*, **36**, 1609 (2002).
61. Z. Tan, J. Qiu, H. Zeng, H. Liu and J. Xiang, *Fuel*, **90**, 1471 (2011).
62. J. Goel, K. Kadirvelu and C. Rajagopal *Adsorpt. Sci. Technol.*, **22**, 257 (2004).
63. D. Pathania, R. Katwal, G. Sharma, M. Naushad, M. R. Khan and A. H. Al-Muhtaseb, *Int. J. Biol. Macromol.*, **87**, 366 (2016).
64. R. Katwal, H. Kaur, G. Sharma, M. Naushad and D. Pathania, *J. Ind. Eng. Chem.*, **31**, 173 (2015).